THE CONDUCTIVITY OF A NANOWIRE: QUANTUM AND LOCALIZATION REGIMES

JJ. PASCUAL, J. GÓMEZ-HERRERO, J. MÉNDEZ AND A.M. BARÓ
Departamento de Física de la Materia Condensada Universidad Autónoma de Madrid. E-28049 MADRID (SPAIN)

N. GARCÍA
Departamento de Física de la Materia Condensada, Física de Pequeños Sistemas, CSIC. Universidad Autónoma de Madrid. E-28049 MADRID (SPAIN)

AND

UZI LANDMAN, W.D. LUEDTKE, E.N. BOGACHEK AND H.P. CHENG
School of Physics, Georgia Institute of Technology, Atlanta, GA 30332

Abstract. Measurements of room temperature electronic transport in pulled metallic nanowires are presented, demonstrating that the conductance characteristics depend on the length, lateral dimensions, state and degree of disorder, and elongation mechanism of the wire. Conductance during elongation of short wires, exhibits periodic quantization steps with characteristic dips, correlating with the order-disorder states of layers of atoms in the wire, predicted via molecular dynamics simulations. The resistance of long wires, as long as 1 - 400 Å, exhibits localization characteristics with $\ln R(l) \sim l^2$

1. Introduction

Material systems of reduced size and/or dimensionality may, and often do, exhibit properties different from those found in the bulk. These include: quantized conductance [1, 2] in point contacts and narrow channels whose characteristic (transverse) dimensions approach the electronic wave length, localization phenomena in low dimensional systems [3], and mechanical properties characterized by a reduced propensity for creation and propagation of dislocations in small metallic samples [4, 5]. Such phenomena are of significant scientific and technological interest, particularly in the area of miniaturized, highly compact, electronic devices.

Most studies of electronic transport phenomena in micro-constrictions are currently performed on high-purity two-dimensional (2D) electron gas systems having a large Fermi-wavelength ($\lambda_F \sim 400$ Å), and are conducted at cryogenic conditions [2]. In contrast, our focus here is on room-temperature transport in three-dimensional (3D) metallic nanowires with $\lambda_F \sim 5$ Å. In such systems, where the width of the constriction is of the order of λ_F , the atomic-scale structure, imperfections, impurities and diffusive boundary scattering are expected to play an important role. Nevertheless, measurements at room-temperature exhibiting conductance quantization were reported recently [6] on short gold nano-wires (~ 40 Å) using a scanning tunneling microscope (STM). Additional observations of quantized conductance steps [1, 2][7]-[10] in short wires [11]-[13], as well as formation of long lead wires at elevated temperatures [14], have been reported. Such observations have been attributed to changes in the contact area during the elongation process of the wire [5, 15], and/or to a decrease in the number of transverse modes (channels) in the stretched junction [6], irrespective of the nature of the elongation mechanism [12].

In this letter we investigate the evolution of room- temperature electronic transport properties in gold nano-wires, from quantized conductance (in $2e^2/h$ or $2(2e^2/h)$ steps with a spatial periodicity of ~ 2 Å) during elongation of short (~ 50 Å) wires, to the onset of localization in long ($100 \text{ Å} \leq l \leq 400$

Å) ones. Moreover, the combination of electronic conductance measurements with MD simulations of the wire elongation process, allows us to elucidate the physical origins of the observed patterns. For short wires, the periodic occurrence of quantized conductance, accompanied by characteristic "dips" (local conductance minima associated with the presence of disorder [16]), are correlated with atomic-scale structural transformations occurring during the layer-by-layer order-disorder elongation process. The dominance of disorder and onset of localization in long wires (longer than the localization length) are portrayed by a nonlinear dependence of the resistance, *R*, on the length of the wire as it is pulled continuously (i.e., $\ln R(l) \sim l^2$). Additionally, current versus voltage data, recorded at selected stages of the elongation process, indicate gradual loss of metallic character as the long wire narrows.

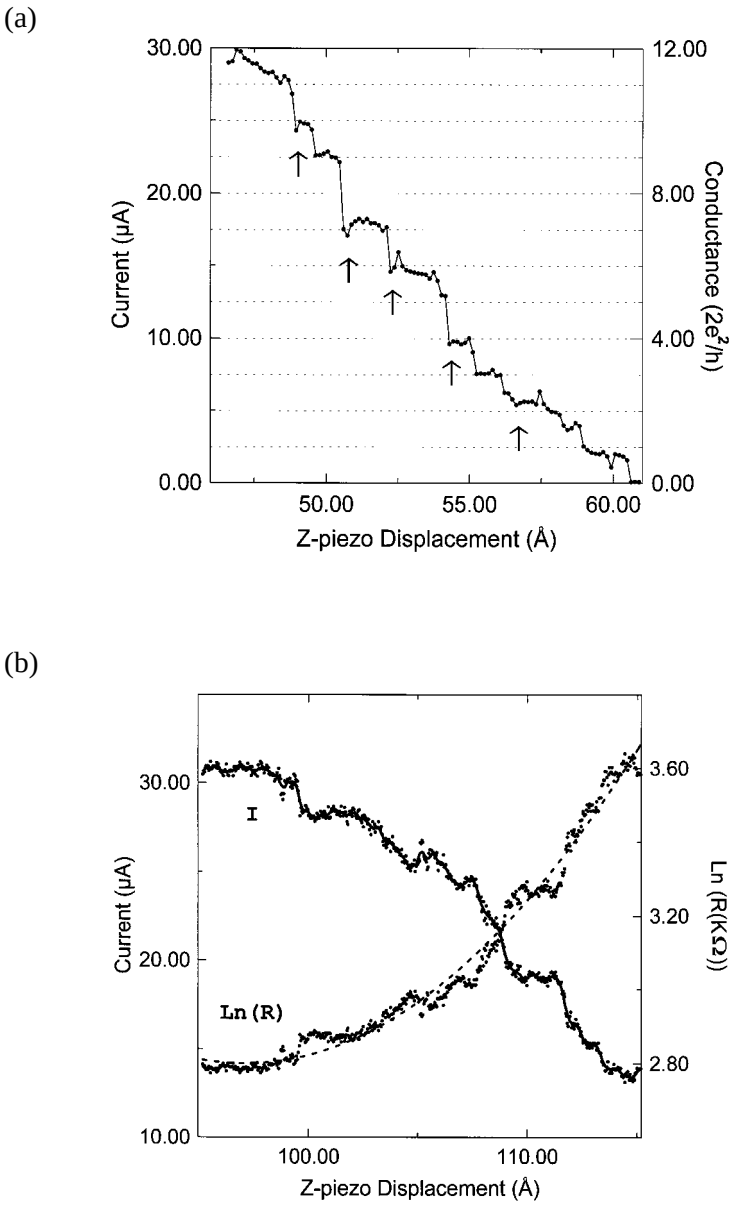

Figure 1. (a) Current and conductance of a shorter wire during an elongation process measured at room temperature, exhibiting conductance quantization steps. Horizontal dashed lines denote intervals of $2e^2/h$. Arrows point to dips interpreted as disordering stages in the elongation process. (b) Left scale: The current in a 95Å wire as it is pulled for 20Å more until breaking. A voltage of 500 mV was applied in the measurement. Smoothed line is introduced for clarity. Right scale: natural logarithm of the resistance of the wire during the elongation process. The solid line corresponds to $\ln R = a + b(z\text{-}z_0)^2$ with $a = 2.8$, $b = 2.6 \times 10^{-3}$ and $z_0 = 97$ Å.

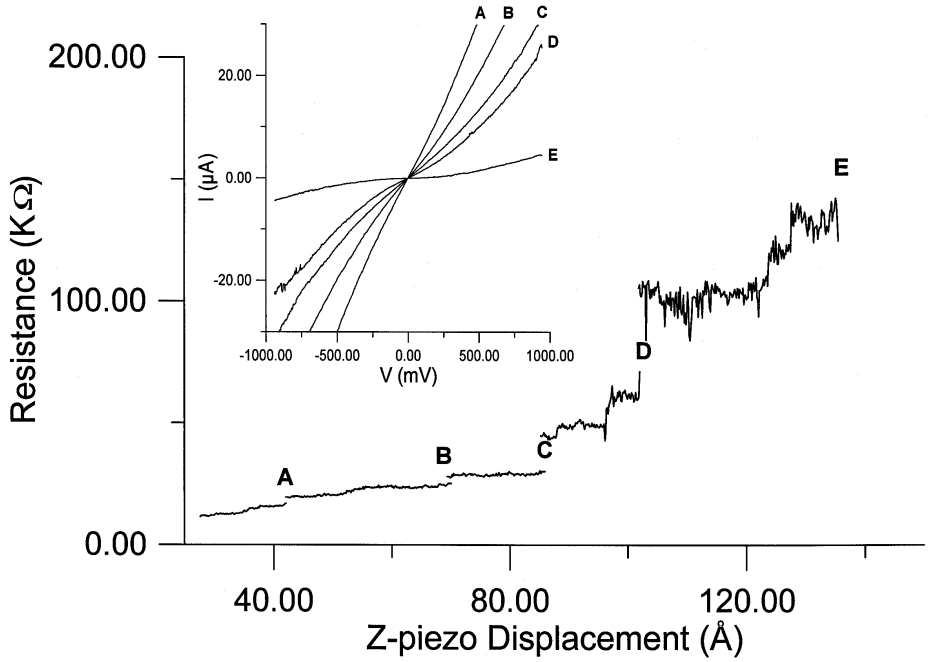

Figure 2. Resistance versus elongation of a wire pulled up to 185Å in total. The process was stopped at 5 places to measure the I-V spectra shown in the inset. The retraction was done at a constant speed of the order of 1Å/s while applying a constant voltage of 100 mV. Letters indicate the stopping points where the I-V data was acquired (ten such measurements were performed at each point). The discontinuities after I-V measurements may be due to some changes in the wire during the experiment.

2. Experimental

In our experiment, contact between the tip and the substrate is produced either by applying a voltage pulse or by indentation, starting from typical STM tunnel conditions. Once the contact is produced as indicated by the electrical current flowing between the two electrodes, we elongate it by retracting slowly the tip (~ 1 Å/s). To achieve optimal control over the STM operations we have developed a digital control unit which allows us to break the feedback loop at any prescribed time and act on the z-piezo. Experiments were carried out at room temperature using home-made STM heads, operating either under ambient conditions or at UHV. Gold evaporated onto mica and Au(110) single crystals were used as samples, and Pt/Ir and gold tips were employed interchangeably (our results are insensitive to the kind of tip used; probably the Pt/Ir tip apex is covered with gold atoms once the tip touches the sample). Since the wires axe more easily formed in air, the data presented in this paper were measured under ambient conditions. However, similar results were obtained in UHV.

3. Results and Discussion

Typical data are shown in Fig. 1a for the conductance of a short wire (~ 50 Å) produced by bringing a Pt/Ir tip to contact with a gold surface in air at room temperature and subsequently elongating slowly the contact by retracting the tip (a constant bias voltage of 32 mV was applied during the process). The voltage was kept constant by using a low gain I-V converter as explained in [6]. We observe that the conductance exhibits quantized steps in one or two units of $2e^2/h$ and that the elongation interval between successive steps is either ~ 2 Å or is split into two intervals whose combined length is ~ 2 Å. Furthermore we call attention to the minima (dips) accompanying the quantized jumps (see discussion bellow).

Next we present data for a long wire which was produced by elongation of the contact for 95 Å under a constant bias voltage of 500 mV. At this point the long wire having a contact resistance of 15 KΩ was pulled further for an additional 20 Å until it broke (Fig. 1b). It is interesting to note the high values of the contact resistance reached which in the case of the data shown in figure 1b increases from 16 KΩ to 37 KΩ. These values are considerably higher than 12.9 KΩ, the resistance of one quantum conductance channel. For the data shown in Fig. 2, where a resistance as high as 150 KΩ was reached, a Pt/Ir tip was retracted for 185 Å before breaking occurred, while applying a bias voltage of 100 mV. In this experiment we have stopped the elongation process at 5 different values of the wire resistance in order to perform fast (~ 0.1 s) measurements of I-V chaxacteristics (Fig. 2).

The observed voltage dependence of the current through the wire (Fig. 2, inset) indicates a transition from a metallic, linear character for long wires with a large cross-sectional area (lower resistance), to a semi-conducting or insulating-like regime for longer and narrower wires. While further studies of this behaviour are necessary, we suggest that these observations may imply Coulomb charging and/or the increasing importance of electron-electron correlations as such long wires become thinner, possibly leading to the appearance of conductivity gaps.

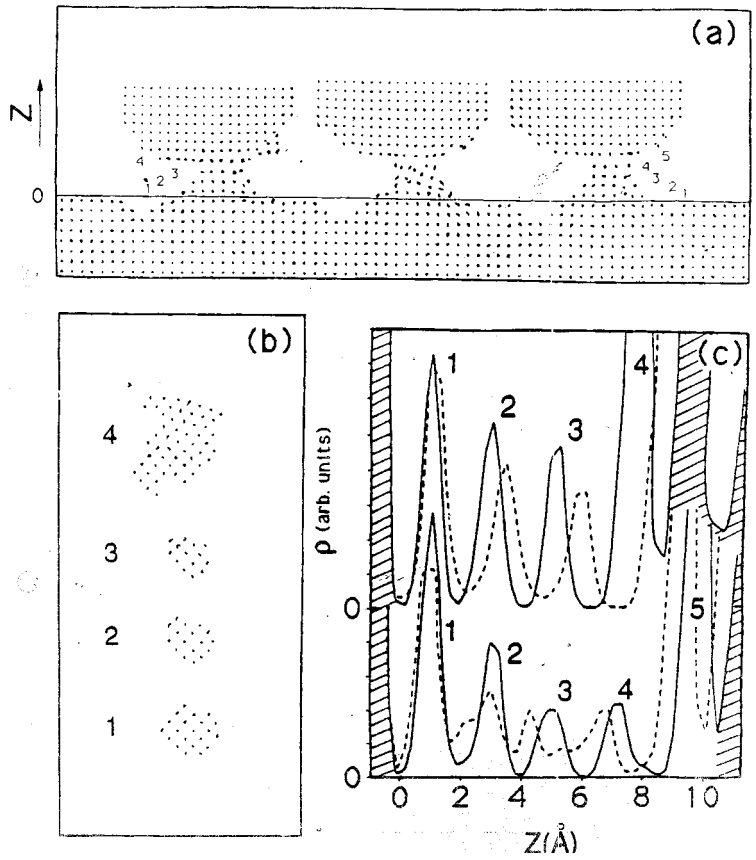

Figure 3. (a) Side views of atomic configurations obtained from short-time trajectories during a MD simulation of a Ni tip slightly indented into, and then retracted from, an Au(001) surface at 300 K. On the left, a 4-layer ordered gold junction formed between the tip and the substrate (the 4th layer of the junction coats the bottom of the tip); the middle configuration demonstrates disorder in the junction during elongation, culminating in the 5-layer ordered junction shown on the right. (b) Top views of the in-layer atomic arrangements corresponding to a 4-layer ordered wire. (c) Profiles of atomic densities plotted versus distance (Z) along the axis of the wire. The solid lines at the top and bottom correspond to the 4-layer and 5-layer ordered junctions respectively (i.e., left and right configurations in (a)). The dashed line at the top part corresponds to a 4-layer strained configuration and the one at the bottom to the disordered structure (middle configuration in (a)) which developed during the elongation process. Hatched regions represent Au substrate ($Z \leq 0$) and Ni tip layers.

To discuss the origins of these experimental results we correlate them with extensive MD simulations, where retraction of a tip from a gold surface after contact resulted in the formation of a solid gold junction [5]. The elongation of the junction in response to the applied external pulling force, at room temperature, consists of a sequence of step-wise elongations stages. In each elongation stage, atoms in layers (mainly in the vicinity of the narrowest part of the junction) respond first via accumulation of stress accompanied by the occurrence of strained configurations of the wire (which remains ordered in atomic layers, though with increasing non-uniformity of the interlayer spacings). This stage is followed by a shorter atomic disordering and rearrangement period culminating in the formation of an added layer, with a relief of the accumulated stress and restoration of a higher degree of order in the wire. Consequently each such elongation-necking stage results in a more extended crystalline junction (in increments of the order of the interlayer spacing in the junction, i.e., ~ 2 Å) of a smaller cross-sectional neck area (see Fig. 3a,b). We remark that in these simulations the overall translation of the tip was performed in an "adiabatic" manner allowing for dynamical structural relaxations throughout the elongation process. Failure to allow for such relaxations may result in a sequence of disordered, and/or melted structures.

To illustrate the elongation process we show in Fig. 3a side views of atomic configurations (recorded in a simulation [5]-a of a Nickel tip interacting with an Au(001) surface, modelled by many-body embedded atom potentials), starting from a layer-ordered junction containing 4 atomic layers (see the corresponding intra-layer atomic arrangements shown in Fig. 3b) and ending with a longer layer-ordered junction containing 5 layers, along with a structure during the intervening disordering stage. Corresponding plots of the atomic density profiles along the normal axis (Z) of the junction shown in Fig. 3c illustrate the atomic distributions in the initial and final ordered stages of the junction as well as during the straining and disordering stages of the transformation.

During the elongation process the wire evolves through atomic configurations with various degrees of order and disorder. We also note that even at the ordered stages, which exhibit crystalline like atomic layers along the axis of the junction, the shapes (peripheries) of the layers are rather irregular (see Fig. 3b), resulting in a solid wire with a surface roughness of a few angstroms, comparable to the wavelength of the electrons (~ 4 Å). While such aspect of disorder may not affect largely the mechanical characteristics it can influence electronic transport processes.

The appearance of room-temperature quantized conductance in the short wires and its persistence (see Fig. 1a where 9 steps of height $2e^2/h$ or $2(2e^2/h)$, with a period d ~ 2 Å, the interlayer spacing in the material, are seen) are quite remarkable, particularly in view of the known sensitivity of conductance quantization to the presence of disorder (which in our wires includes surface roughness, and disorder occurring between the intermittent layer-ordered stages, see Fig.3). This implies that overall, wires in this length regime maintain a sufficient degree of crystalline order (see Fig. 3) to sustain quantization of the conductance. Furthermore, significant insigths into the microscopic mechanism of the elongation process and nature of disorder in the wire are provided by the observation of dips accompanying the quantized conductance steps (see Fig. 1a), which can be associated with electron scattering caused by the enhanced structural disorder developing toward the completion of each of the discrete elongation stages of the wire. The rapid rise in the conductance following each dip indicates restoration of a higher degree of order in the pulled wire subsequent to the disordering-rearrangement elongation stage (notice also the small spikes in Fig. 1a). In addition, the variability in the conductance quantization step-height (one or two $2e^2/h$ units) and the above-mentioned occasional occurrence of two successive steps in an elongation interval of combined length ~ d (see Fig. 1a), may originate from accidental degeneracies of the (2D) transverse electronic states, irregular shapes of the layers in the wire, and most likely the occurrence of intermediate atomic configurations during the elongation process which satisfy the condition for closing of a conductance channel. These observations support a correlation between the measured patterns and the aforementioned periodic layer-wise order-disorder elongation mechanism of the wire.

In contrast, conductance quantization was not observed during elongation of long wires ($l \geq 100$ Å see Fig. 1b). For such long quasi one-dimensional wires, were the resistance reaches values much higher than the quantum unit of resistance, one may expect signatures of Anderson localization [3], if the length of the wire l exceeds the localization length L, implying an exponential growth of the

resistance R with l, i.e., $R(l) \sim \exp(l/L)$. However, the data shown in figure 1 shows a quadratic behaviour instead of linear. We interprete this as a consequence of variations of the localization length L as the wire is continuously pulled. Using the expression for L from [17] $L \sim Sk_F^2\lambda$, where S is the cross-sectional area of

However, since the wire is being continuously pulled, the value of L may vary, depending on the elongation. The localization length is given by [17] $L \sim Sk_F^2\lambda$ where S is the cross-sectional area of the wire, k_F is the Fermi wave vector, and A the elastic mean free path. Since the volume Ω of the wire remains constant during room-temperature elongation (as observed in MD simulations [5]), S decreases with increasing l (e.g. for a cylindrical wire $S = \Omega/l$). Using this in $\exp(l/L(l))$ leads to a non-linear dependence, $\ln R(l) \sim l^2$. Indeed, such dependence of the measured resistance on l is depicted in Fig. 1b, (values of $L \leq 40$ Å may be estimated from this data).

In summary, our studies reveal that the room temperature electronic transport properties in pulled metallic (Au) nanowires evolve as a function of length, from conductance quantization in steps of one or two $2e^2/h$ units, occurring with an approximate period of the interlayer spacing and accompanied by conductance dips, for short wires ($l \sim 50$ Å), to a localization regime with $\ln R(l) \sim l^2$ for wires whose length ($l \geq 100$ Å) exceeds the localization length. These observations correlate with the results of MD simulations.

Useful discussions with J.J. Sáenz and experimental software support by J.M. Gómez-Rodrígez are acknowledged. J.I.P, J.M., J.G-H. and A.M.B. acknowledge financial support by CICYT under project No. PB92-0158. N.G. acknowledge CICYT projects MAT 92-0129. The work of U.L., W.D.L., E.N.B. and H.P.Ch. is supported by the U.S. Department of Energy Grant no. DE FG05-86ER45234.

References

1. R. Landauer, J. Phys: Condens. Matter **1**, 8099 (1989).

2. "Nanostructure Physics and Fabrication", eds. M.A. Reed and W.P. Kirk. (Academic, San Diego, 1989); C.W.J.Beenakker and H. van Houten, Solid State Physics **44**, 1 (1991).

3. P.W. Anderson, Phys. Rev. **109**, 1492 (1958); P.A. Lee and T.V. Ramakrishnan, Rev. Mod. Phys. **57**, 287 (1985).
4. R.W. Siegel, Mat. Sci. Eng. B **19**, 37 (1993).

5. a) U. Landman, W.D. Luedtke, N.A. Burnham and RJ. Colton, Science **248**, 454 (1990); b) U. Landman and W.D. Luedtke, J. Vac. Sci. Tech. **9**, 414 (1991).

6. JJ. Pascual, J. Méndez, J. Gómez-Herrero, A.M. Baró, N. García and Vu Thien Binh, Phys. Rev. Lett. **71**, 1852 (1993).

7. N. García and L. Escapa, Appl. Phys. Lett. **54**, 1418 (1989); N. García, presentation at STM Workshop, ITCP (Trieste) 1987,
unpublished.

8. S. Ciraci and E. Tekman, Phys. Rev. Lett. **62**, 1860 (1989).

9. E.N. Bogachek, A.M. Zagoskin, and I.0. Kulik, Sov. J. Low. Temp. Phys. **16**, 796 (1990).

10. J.A. Torres, J.J. Pascual and J.J. Sáenz, Phys. Rev. B **49**, 16581 (1994).

11. N. Agrait, J.G. Rodrigo, and S. Viera, Phys. Rev. B **47**, 12345 (1993).

12. L. Olesen, E. Laegsgaard, I. Stensgaard , F. Besenbacher, J. Schiøtz, P. Stoltze, K.W. Jacobsen, and IN. Nørskov, Phys. Rev. Lett. **72**, 2251 (1994).

13. J.M. Krans, C.J. Muller, I.K. Yanson, Th.C.M. Govaert, R. Hesper, and J.M. van Ruitenbeek, Phys. Rev. B **48**, 14721 (1993).

14. L. Kuipers and J.W.M. Frenken, Phys. Rev. Lett. **70** , 3907 (1993).

15. T.N. Todorov and A.P. Sutton, Phys. Rev. Lett. **70**, 2138 (1993).

16. I. Kander, Y. Imry, and U. Sivan, Phys. Rev. B **41**, 12941 (1990); Th.M. Nieuwenhuizen, Europhys. Lett. **24**, 269 (1993).

17. D.J. Thouless, Phys. Rev. Lett. **39**, 1167 (1977).